

Automatic Diagnosis of High-Resolution Esophageal Manometry using Artificial Intelligence

Stefan Lucian Popa¹, Teodora Surdea-Blaga¹, Dan Lucian Dumitrascu¹, Giuseppe Chiarioni², Edoardo Savarino³, Liliana David¹, Abdulrahman Ismaiel¹, Daniel Corneliu Leucuta⁴, Imre Zsigmond⁵, Gheorghe Sebestyen⁶, Anca Hangan⁶, Zoltan Czako⁶

1) 2nd Medical Department, Iuliu Hatieganu University of Medicine and Pharmacy, Cluj-Napoca, Romania; 2) Division of Gastroenterology of the University of Verona, AOUI Verona, Verona, Italy; 3) Division of Gastroenterology, Department of Surgical, Oncological and Gastroenterological Sciences, University of Padua, Padua, Italy; 4) Department of Medical Informatics and Biostatistics, Iuliu Hatieganu University of Medicine and Pharmacy, Cluj-Napoca, Romania; 5) Faculty of Mathematics and Computer Science, Babes-Bolyai University, Cluj-Napoca, Romania; 6) Department of Computer Science, Technical University of Cluj-Napoca, Cluj-Napoca, Romania

ABSTRACT

Background & Aims: High-resolution esophageal manometry (HREM) is the gold standard procedure used for the diagnosis of esophageal motility disorders (EMD). Artificial intelligence (AI) might provide an efficient solution for the automatic diagnosis of EMD by improving the subjective interpretation of HREM images. The aim of our study was to develop an AI-based system, using neural networks, for the automatic diagnosis of HREM images, based on one wet swallow raw image.

Methods: In the first phase of the study, the manometry recordings of our patients were retrospectively analyzed by three experienced gastroenterologists, to verify and confirm the correct diagnosis. In the second phase of the study raw images were used to train an artificial neural network. We selected only those tracings with ten test swallows that were available for analysis, including a total of 1570 images. We had 10 diagnosis categories, as follows: normal, type I achalasia, type II achalasia, type III achalasia, esophago-gastric junction outflow obstruction, jackhammer oesophagus, absent contractility, distal esophageal spasm, ineffective esophageal motility, and fragmented peristalsis, based on Chicago classification v3.0 for EMDs.

Results: The raw images were cropped, binarized, and automatically divided in 3 parts: training, testing, validation. We used Inception V3 CNN model, pre-trained on ImageNet. We developed a custom classification layer, that allowed the CNN to classify each wet swallow image from the HREM system into one of the diagnosis categories mentioned above. Our algorithm was highly accurate, with an overall precision of more than 93%.

Conclusion: Our neural network approach using HREM images resulted in a high accuracy automatic diagnosis of EMDs.

Key words: artificial intelligence – convolutional neural network – Chicago classification – esophageal motility disorder diagnosis – high-resolution esophageal manometry – machine learning.

Abbreviations: AI: artificial intelligence; CNN: convolutional neural networks; DL: deep learning; EMD: esophageal motility disorders; HREM: high resolution esophageal manometry; IRP: 4s-integrated relaxation pressure; LES: lower esophageal sphincter.

Address for correspondence:

Teodora Surdea-Blaga
2nd Medical Department,
Iuliu Hatieganu University of
Medicine and Pharmacy,
Cluj-Napoca, Romania

Received: 31.07.2022
Accepted: 27.10.2022

INTRODUCTION

High-resolution esophageal manometry (HREM) is the gold standard procedure used for the diagnosis of esophageal motility disorders (EMD) [1, 2]. High-resolution esophageal manometry employs solid-state or water-perfused catheters with up to 36 circumferential sensors that provide color pressure topography maps that depict the pressures created in the

esophageal body because of muscle contractions during swallowing [1, 2].

The diagnosis of EMDs is based on a Chicago classification algorithm [2], using different parameters, including the 4s-integrated relaxation pressure (IRP), distal latency and distal contractile integral. All these parameters are returned automatically by the software, but they require human intervention for the correct positioning of the different markers in the HREM plots. For example, upper and lower borders of the lower esophageal sphincter (LES) are established by the physician, and the presence of a hiatus hernia (i.e. a clear separation between the LES and crural diaphragm, the two anatomic components constituting the esophagogastric junction) makes things more difficult. The contractile

deceleration point [3], a marker used to determine distal latency which makes the difference between normal and spastic swallows, is another marker on the HREM recording that is operator dependent. Inevitably, this may lead to intra and inter-observer variability [4, 5], leading in some cases to a different diagnosis, and thus inappropriate treatment recommendations. One study reported a moderate overall inter-observer agreement ($\kappa=0.51$), with higher values for type I and II achalasia ($\kappa > 0.7$), and smaller for any diagnosis ($\kappa=0.34$). The overall agreement varied with the number of studies performed by the physician [4], so the experience of the physician is another important parameter that may influence the final diagnosis. Hence, despite the available algorithm, different physicians would establish a different final diagnosis on the same tracing [1, 2].

In several application fields, automated image processing and computer vision have gained immense appeal in recent years (e.g., medicine, industry, autonomous driving, robotics, etc.). This is largely a consequence of recent breakthroughs in a variety of computer vision-related tasks, including image classification, image segmentation, object identification and detection, 3D scene reconstruction, etc. Deep learning (DL) methods, including convolutional neural networks (CNN), virtually always provide high-quality results [6].

Deep learning, a subset of artificial intelligence (AI) techniques, has transformed the image processing industry. The availability of high-performance computing infrastructures (e.g., parallel computers, cloud systems, GPUs, multi-core processors, etc.) plus the accessibility of vast quantities of publicly available data make DL a viable solution in a variety of domains [6].

Deep learning might provide a viable answer to improve HREM's subjective interpretation problems because a significant quantity of raw manometry data paired with neural networks might be utilized to detect the distinct patterns that differentiate EMDs [6]. Deep learning-based systems were applied in different fields of gastroenterology, such as in colon polyps' detection, digital pathology or for the assessment of radiological images, assessment of liver fibrosis, or differentiation of pancreatic cancer from chronic pancreatitis [6].

Given the high amount of data from pressure variations in time, HREM is another field in gastroenterology, in which a DL-based system, able to perform a completely automatic analysis of manometry tracings, would facilitate data interpretation and represent a cost-efficient future perspective [7, 8]. A DL system might be taught to diagnose EMDs based on raw manometry images. In this way, even in the absence of an available physician specialized in manometry interpretation, one can have a rapid prediction/or a rapid diagnosis of the motility disorder, if any. Therefore, our study aimed to develop a DL-based system, using neural networks, for the automatic diagnosis of HREM images. Our system did not use any manometry parameters (that are part of the Chicago algorithm, like IRP, DL, etc.) instead, it used as the input raw manometry images. We used a CNN such as InceptionV3 [9, 10] for feature extraction and a custom made fully connected layer for classifying these features into 10 esophageal disorder classes. More specifically we trained and tested a pre-trained

InceptionV3 CNN to be able to classify one wet swallow raw image of HREM into ten esophageal disorder classes.

METHODS

This study was retrospective. We used our manometry database, which included manometry tracings performed at our department, between November 2014 and February 2021, in a regional tertiary hospital. The Ethics Committee of the University of Medicine and Pharmacy, Cluj-Napoca approved the study (11900/27.04.2021).

High Resolution Esophageal Manometry Procedure

The HREMs with pressure topography were performed after 8-h fasting, using the ISOLAB manometry system (Standard Instruments, Germany). The system used solid-state probes, with 36 circumferential sensors, spaced at 1 cm. The probe was placed trans-nasally, with at least 3 sensors in the stomach, and the test was performed with the patients in supine position, with the thorax angulated at 30°. Ten wet swallows, 5 ml each were performed. For each test swallow, a marker, represented by a white vertical line ("wet swallow" marker), was placed during the recording, by the examiner, to later differentiate wet from dry swallows. Only wet swallows were analyzed. All the tracings were analyzed by one gastroenterologist specialized in HREM interpretation (T.S.-B.). The swallows were analyzed, and a conclusion for each study was established, based on Chicago v 3.0 classification. Between March and May 2021, we screened our manometry database, and we selected the studies that had 10 correct test swallows, to create the image database. Traditionally, at least 10 wet swallows are considered sufficient to assess the esophageal motility. Therefore, studies with 7-9 correct swallows were excluded.

The classifications in the study cohort were retrospectively analyzed by other two experienced motility experts (G.C. and E.S.), to verify and confirm the correct diagnosis. In cases of disagreement, consensus was established after analyzing together the recordings.

For each included study, only one EMD was established. Changes of the upper esophageal sphincter, presence of hiatal hernia or hypertensive LES were not assessed. Studies who did not fit well into one Chicago classification category were excluded (for example, esophago-gastric outflow obstruction criteria with hypertensive peristalsis-jackhammer esophagus, in the same patient). To classify the studies, we used the Chicago v3.0 algorithm [2]. We used Unisensor® catheter, and the upper normal limit of 4s-IRP was set at 28 mmHg. Achalasia diagnosis was established when 4s-IRP was ≥ 28 mmHg and one of the following criteria was present: a. absence of peristaltic waves in 100% of swallows for type I achalasia; b. pan-esophageal pressurization in $\geq 20\%$ of swallows and no peristaltic waves- for type II achalasia; c. abnormal peristaltic waves, with $\geq 20\%$ spastic waves for type III achalasia. Studies with a normal median 4s-IRP, pan-esophageal pressurization in $\geq 20\%$ of swallows and no peristaltic waves, were classified as type II achalasia. Studies with the same criteria as the latter, and at least 1 swallow followed by pan-esophageal pressurization, were classified as type I achalasia [2]. Studies with normal median 4s-IRP, absence of peristaltic waves

and no pressurization were classified as absent contractility, irrespective of other clinical, endoscopic, or radiological data we might have had regarding the patients. Other studies with increased median 4s-IRP (≥ 28 mmHg) and no criteria for achalasia, were classified as esophago-gastric junction outflow obstruction. The other diagnosis (distal esophageal spasm, jackhammer esophagus, ineffective motility, fragmented peristalsis, normal manometry) were also established according with Chicago criteria v3.0 [2].

Creation of Image Dataset

We selected only those tracings with ten test swallows that were available for analysis (n=157 patients; a total of $157 \times 10 = 1570$ images): Achalasia Type I -46 patients, Achalasia Type II - 34 patients, Achalasia Type III - 3 patients, Jackhammer Esophagus - 1 patient, Ineffective Esophageal Motility - 22 patients, Absent Contractility - 12 patients, Fragmented Peristalsis - 3 patients, Distal Esophageal Spasm - 1 patient, EGJ Outflow Obstruction - 10 patients, Normal Esophageal Motility - 25 patients. We used the raw data, containing only the markers mentioned above (vertical white line), before each of the wet swallows. The manometry software allowed to store 60s long images of the recording, and these represented the raw images. The region of interest (the wet swallow) was marked by a white vertical line, placed during the procedure. For each patient we created a folder with 10 images, each image representing a test swallow.

Each set was then included in one diagnosis category. We had 10 diagnosis categories, as follows: normal, type I achalasia, type II achalasia, type III achalasia, esophago-gastric junction outflow obstruction, jackhammer esophagus, absent contractility, distal esophageal spasm, ineffective esophageal motility, and fragmented peristalsis, based on Chicago v3.0 of classification for EMDs [2].

Metrics

In this paper, we used a variety of measurement criteria to provide a comprehensive picture of our approach. These metrics were the following:

- Accuracy: The number of correctly classified HREM images divided by the total number of images. $\text{Accuracy} = (\text{TP} + \text{TN}) / \text{Total image count}$, where TP: true positives and TN: true negatives;
- Precision: The number of correct predictions over the number of correct and in-correct predictions. $\text{Precision} = \text{TP} / (\text{TP} + \text{FP})$, where FP: false positives;
- Recall: The number of correct predictions over the number of all predictions. $\text{Recall} = \text{TP} / (\text{TP} + \text{FN})$, where FN: false negatives;
- F1-Score: harmonic mean of Recall and Precision. $\text{F1-Score} = 2 * [(\text{Precision} * \text{Recall}) / (\text{Precision} + \text{Recall})]$;
- Confusion Matrix: a summary of the classification task, showing the number of correct and incorrect predictions for each class.

The metrics presented above (except the confusion matrix) were calculated per class of images and the overall evaluation metric is the average of them.

Image Pre-Processing

The raw images had more information than needed to train an artificial neural network. The region of interest was represented by a part of the raw images (10-20 seconds from the 60s images, after the white line). Therefore, we cropped the raw images to remove the unnecessary part, called “the noise”. We used this rule: the upper, lower, and right borders were the image borders, and the left border was shown by the white vertical line before each test swallow.

In Fig. 1, we used a black rectangle to highlight an area of interest. To make it easier for the computer to find this area, we removed the gray margins from the top, bottom, and left. This technique was already presented in one of our previous papers [8].

To find the white line that marks the wet swallow, we binarized the image. This resulted in the image shown in Fig. 2. In the next step, to find the vertical white line, we have counted the pixels on the y-axis and chosen the index of the number with the most pixels on it. In the following step in image processing the original picture was cropped using the previously discovered x-position.

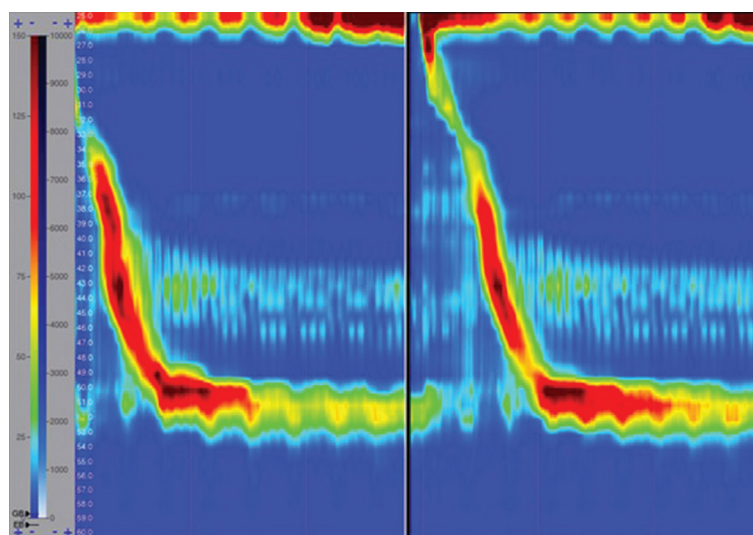


Fig. 1. Raw image with the highlighted region of interest.

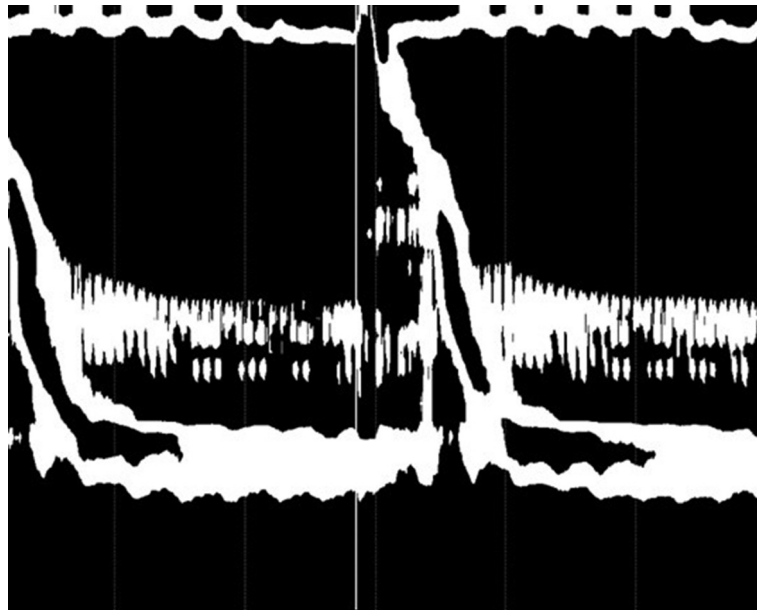


Fig. 2. Binarized image.

Images were rescaled and normalized to have values between -1 and 1 since the CNN that we used for classification has an input shape of 299x299, which works with values between -1 and 1 [8]. Once all the pixel values had been standardized to [-1, 1], they were input into the feature extraction process.

Data was divided into three parts: one for training (70%, 1100 images), another one (15% - 235 images), and a third one (15% - 235 images) for testing and validation. We acquired reliable assessment ratings by using three separate datasets that ensured the model has never seen the test set.

To develop the final model, the CNN model must be trained several times (using the training dataset) while receiving interim input on its quality using the test dataset. The intermediate input is utilized during the training phase to improve the model. Following the completion of the model, the validation dataset is utilized to validate the findings. Having

three independent datasets ensures that the validation set is never available to the model, enabling reliable assessment scores to be generated. The training set contains the bulk of the necessary training data. The test set is used during training to assess the model's ability to interpret pictures it has never seen before. Since the test set is actively used in model building and training, it is essential to retain a distinct dataset. At the completion of the research, assessment metrics were used to the validation set to determine how well the model would perform in the actual world.

Transfer Learning

To train a CNN from scratch, it would be necessary to gather a huge number of tagged medical pictures. Transfer Learning is an effective method for dealing with tiny data [9]. Our starting point in Transfer Learning for the classification of HREM images was another model that had been developed

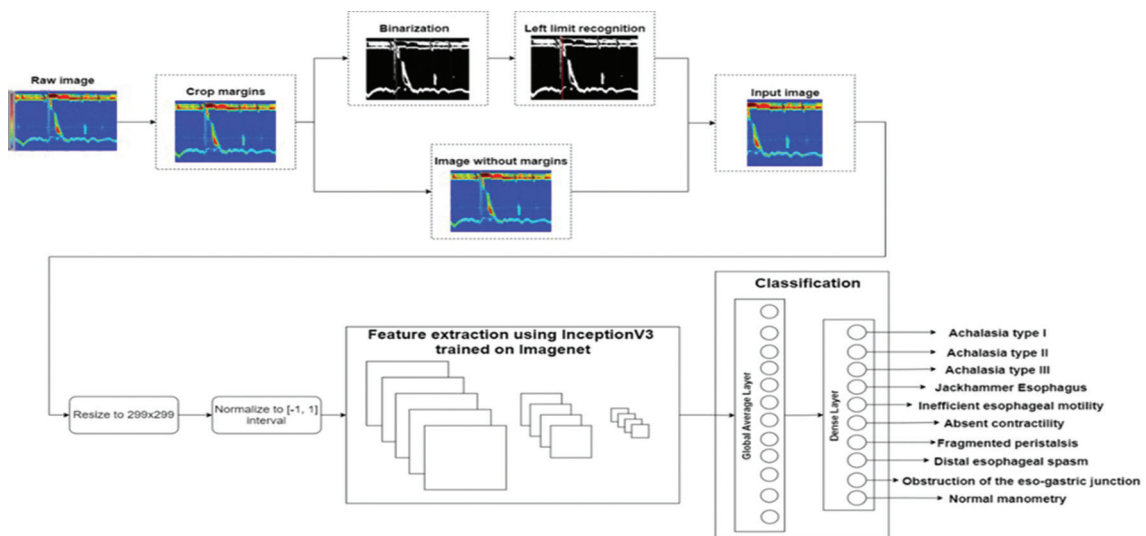


Fig. 3. Solution architecture.

to deal with another classifier issue for which there was a substantially larger amount of labeled training data. Pre-trained on ImageNet, the InceptionV3 the CNN model was utilized in our approach. More than a hundred thousand photos are organized into 1,000 distinct classifications in the ImageNet dataset [10].

Solution Architecture

To finish, we developed a custom classification layer using a Global Average Layer with a dropout of 20% to minimize overfitting issues, as well as a final fully connected layer comprising 10 neurons for each of our 10 classes. With a batch size of 32 pictures and a randomized data set for each epoch, the model was trained using Adam optimizer [11].

RESULTS

For each wet swallow image from the HREM system from the test set the CNN classified it into 10 diagnosis categories. Those were compared with the correct diagnosis and the precision, recall and F1-Score were computed and displayed in Table I. To reach these findings, the model was fed new test data that it had never seen before.

Table I. Evaluation metrics

Class	Precision	Recall	F1-Score
Achalasia type I	95%	97%	96%
Achalasia type II	100%	80%	89%
Achalasia type III	100%	100%	100%
Jackhammer Esophagus	100%	67%	80%
Inefficient esophageal motility	95%	100%	97%
Absent contractility	100%	86%	92%
Fragmented peristalsis	100%	100%	100%
Distal esophageal spasm	67%	100%	80%
Obstruction of the eso-gastric junction	90%	100%	95%
Normal manometry	94%	99%	97%
Overall	94%	93%	95%

We created a confusion matrix calculated on the test dataset, presented in Fig. 4.

DISCUSSION

The approach for this pilot study was different compared to the common way the diagnosis for EMDs is made using HREM. Normally ten wet swallows are used for a patient by a trained physician to establish the presence of a motility disorder. In our study we assessed the accuracy of a CNN to establish the diagnosis for an EMD, based on a single wet swallow image.

Overall the diagnostic accuracy of the CNN system that makes the diagnosis per one image and which was presented in this paper was very high. The accuracy of this system could be further increased by using 10 images per patient and a voting system. The diagnosis would be chosen by taking the majority vote from the classes identified for each of the 10 images of

a patient. Dwelling into specific diagnosis categories, the interpretation was only fair for some disorders such as type II and type III achalasia. In some cases, the distinction between the two entities might be difficult even by the experienced examiner [4, 5, 13]. Overall accuracy and precision (94%) and recall (93%) with our system were very good and are comparable to other solutions previously published [14-17].

Only a few studies have used AI-based systems for the automatic diagnosis of EMDs. For example, Kou et al. [14] used DL to model swallow-level data, to identify the swallowing type. The results were better for pressurization type (normal, compartmental or panesophageal pressurization), with accuracy of 0.87 for test dataset, compared to the swallow type (accuracy of 0.64 for test dataset) [14]. In another study which combined DL and machine learning [15], the authors developed 3 models based on CNNs. The models were blended, and the best prediction was of 0.92 for the diagnosis of EMDs. Frigo et al. [16], created a database with parameters both from normal manometries, and EMDs. Using a decision support system and based on the similarity between the database and patients' parameters, the correct diagnoses were observed in 86% of cases. In another study [17], the authors tried to make real-time predictions on the the esophageal function. It could be normal, or there could be a minor or a major motility disorder. The solution had a good accuracy (91.3%) in identifying the presence of a motility disorder. However, in this study, the system did not return a final EMD diagnosis.

In one of our previous studies [8], we tried to use AI to fully automate EMDs diagnosis, by splitting the problem in two parts. First, we learned the system to recognize correct versus wrong probe positioning, and to discriminate between normal and high IRP, like a human expert would do in the analysis of the manometry tracings. The accuracy was of 90% [8]. The second step would be to learn the system to recognize different patterns of esophageal peristalsis and based on those to achieve to the final diagnosis. This approach would imitate a human expert, that uses the Chicago algorithm for the diagnosis of EMDs.

Some studies analyzed the efficiency of an AI-based system to automatically analyze pharyngeal changes and the upper esophageal sphincter, trying to differentiate swallowing patterns and to recognize abnormal swallowing. For this reason, those studies cannot be compared to our study, as there was no reference to the clasification of EMD or to the Chicago clasification [18-24].

In this paper, we used another approach. The system was trained with images belonging to 10 different classes, without considering the IRP or peristalsis patterns as in our previous work [8]. The algorithm we developed is highly accurate, with a precision of more than 93%. However, these results are based on a single image analysis, the system predicting in which diagnosis category would the image belong. It is worth noting that after training the CNN with manometry images, the response in the case of new images is almost instantaneous, under 1 second; therefore, the execution time is considerably shorter when using AI.

Our study has some limitations. The exclusion of studies that did not fit well into one Chicago classification category could induce a diagnosis purity bias. Nevertheless, the number

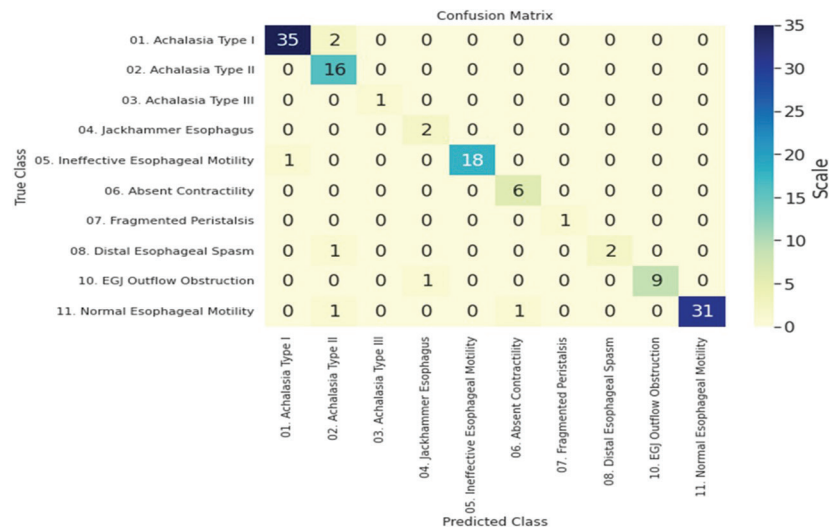


Fig. 4. Confusion matrix.

of these occurrences was small. Moreover, due to the small number of recordings, it was preferred to give clear examples to improve the training of the neural network. Other limitations come from the nature of the images. The image type used by our Neural Networks-based system for training, testing, and validation, may vary significantly depending on the high-resolution manometer device used for recording. Our images were obtained with only one type of device, in one manometry center, so no differences in image type existed, and the outcome was not affected. Another limitation comes from the small number of recordings (a total of 1570 images) used to develop the algorithm. Some of the EMDs (second; therefore, distal esophageal spasm, jackhammer esophagus, fragmented peristalsis) are generally rare in occurrence, and were also quite rare in our cohort, making the number of analyzed images even smaller. In addition, we included in the analysis, only patients with 10 correct swallows. We plan a larger multicentric study, therefore with a higher number of images, and in addition with images obtained with different manometry systems, to see if our solution is still valid. In future projects we intend to test the solution with patients that have more than one disorder according to the Chicago classification. In this study, these patients were excluded.

The tracings were classified based on Chicago classification v3.0, which was available when the tests were performed. The other studies published on this topic, also used this version of the Chicago classification [8, 14-17]. The updated version v. 4.0 has already addressed some of the weakness of the former version [12]. Moreover, the last iteration of Chicago classification set up a brand-new protocol of examination which includes both supine and upright position, administration of a solid meal, and clinical correlates which could not be considered in the actual study. This last version of the Chicago classification has not been implemented in routine clinical practice, yet. In the future, AI will support the integration of information obtained from clinical findings, endoscopy, HREM and endoluminal functional lumen imaging probe, to come to a clinically relevant, yet comprehensive conclusion.

CONCLUSIONS

Our neural network approach using images obtained from HREM can obtain an automatic diagnosis of EMD with high accuracy. Therefore, the implementation of an AI-based algorithm is a useful diagnosis tool, when an experienced physician in manometry is not available.

Conflicts of interest: None to declare.

Authors' contribution: S.L.P., T.S.-B., Z.C., D.C.L., G.S., I.Z., A.H. conceived the study and designed the methodology. T.S.-B., L.D. collected the data acquisition. T.S.-B., G.C., E.S. analyzed the tracing of HREM. S.L.P., T.S.-B., A.I., created the image database. S.L.P., T.S.-B., Z.C. drafted the manuscript. D.L.D., G.C., E.S., L.D., D.C.L., G.S., A.H., A.I., I.Z. wrote the manuscript and revised it critically for important intellectual content. All authors approved the final version of the paper.

Acknowledgements: This paper was financially supported by the Project "Entrepreneurial competences and excellence research in doctoral and postdoctoral programs - ANTREDOC", project co-funded by the European Social Fund financing agreement no. 56437/24.07.2019.

REFERENCES

- Bredenoord AJ, Smout AJ. High-resolution manometry. *Dig Liver Dis* 2008;40:174-181. doi:10.1016/j.dld.2007.11.006
- Kahrilas PJ, Bredenoord AJ, Fox M, et al. The Chicago Classification of esophageal motility disorders, v3.0. *Neurogastroenterol Motil* 2015;27:160-174. doi:10.1111/nmo.12477
- Roman S, Lin Z, Pandolfino JE, Kahrilas PJ. Distal contraction latency: a measure of propagation velocity optimized for esophageal pressure topography studies. *Am J Gastroenterol* 2011;106:443-451. doi:10.1038/ajg.2010.414
- Fox MR, Pandolfino JE, Sweis R, et al. Inter-observer agreement for diagnostic classification of esophageal motility disorders defined

- in high-resolution manometry. *Dis Esophagus* 2015;28:711-719. doi:[10.1111/dote.12278](https://doi.org/10.1111/dote.12278)
5. Kim JH, Kim SE, Cho YK, et al. Factors Determining the Inter-observer Variability and Diagnostic Accuracy of High-resolution Manometry for Esophageal Motility Disorders. *J Neurogastroenterol Motil* 2018;24:506. doi:[10.5056/jnm24031](https://doi.org/10.5056/jnm24031)
 6. Cao JS, Lu ZY, Chen MY, et al. Artificial intelligence in gastroenterology and hepatology: Status and challenges. *World J Gastroenterol* 2021;27:1664-1690. doi:[10.3748/wjg.v27.i16.1664](https://doi.org/10.3748/wjg.v27.i16.1664)
 7. Visaggi P, Barberio B, Gregori D, et al. Systematic review with meta-analysis: artificial intelligence in the diagnosis of oesophageal diseases. *Aliment Pharmacol Ther* 2022;55:528-540. doi:[10.1111/apt.16778](https://doi.org/10.1111/apt.16778)
 8. Czako Z, Surdea-Blaga T, Sebestyen G, et al. Integrated Relaxation Pressure Classification and Probe Positioning Failure Detection in High-Resolution Esophageal Manometry Using Machine Learning. *Sensors (Basel)* 2021;22:253. doi:[10.3390/s22010253](https://doi.org/10.3390/s22010253)
 9. Bengio Y. Deep Learning of Representations for Unsupervised and Transfer Learning. In: Silver DL, Guyon I, Taylor G, Dror G, Lemaire V. Editors. *Proceedings of ICML Workshop on Unsupervised and Transfer Learning; Proceedings of Machine Learning Research*: PMLR; 2012:17-36.
 10. Deng J, Dong W, Socher R, Li LJ, Kai Li, Li Fei-Fei. ImageNet: A large-scale hierarchical image database. *IEEE Conference on Computer Vision and Pattern Recognition*. 2009:248-255. doi:[10.1109/CVPR.2009.5206848](https://doi.org/10.1109/CVPR.2009.5206848)
 11. Kingma DP, Ba JL. A method for stochastic optimization. 2014. Published as a conference paper at the 3rd International Conference for Learning Representations, San Diego, 2015. doi:[10.48550/arXiv.1412.6980](https://doi.org/10.48550/arXiv.1412.6980)
 12. Fox MR, Sweis R, Yadlapati R, et al. Chicago classification version 4.0© technical review: Update on standard high-resolution manometry protocol for the assessment of esophageal motility. *Neurogastroenterol Motil* 2021;33:e14120. doi:[10.1111/nmo.14120](https://doi.org/10.1111/nmo.14120)
 13. Bogte A, Bredenoord AJ, Oors J, Siersema PD, Smout AJ. Reproducibility of esophageal high-resolution manometry. *Neurogastroenterol Motil* 2011;23:e271-e276. doi:[10.1111/j.1365-2982.2011.01713.x](https://doi.org/10.1111/j.1365-2982.2011.01713.x)
 14. Kou W, Carlson DA, Baumann AJ, et al. A deep-learning-based unsupervised model on esophageal manometry using variational autoencoder. *Artif Intell Med* 2021;112:102006. doi:[10.1016/j.artmed.2020.102006](https://doi.org/10.1016/j.artmed.2020.102006)
 15. Kou W, Carlson DA, Baumann AJ, et al. A multi-stage machine learning model for diagnosis of esophageal manometry. *Artif Intell Med* 2022;124:102233. doi:[10.1016/j.artmed.2021.102233](https://doi.org/10.1016/j.artmed.2021.102233)
 16. Frigo A, Costantini M, Fontanella CG, Salvador R, Merigliano S, Carniel EL. A Procedure for the Automatic Analysis of High-Resolution Manometry Data to Support the Clinical Diagnosis of Esophageal Motility Disorders. *IEEE Trans Biomed Eng* 2018;65:1476-1485. doi:[10.1109/TBME.2017.2758441](https://doi.org/10.1109/TBME.2017.2758441)
 17. Wang Z, Hou M, Yan L, Dai Y, Yin Y, Liu X. Deep learning for tracing esophageal motility function over time. *Comput Methods Programs Biomed* 2021;207:106212. doi:[10.1016/j.cmpb.2021.106212](https://doi.org/10.1016/j.cmpb.2021.106212)
 18. Mielens JD, Hoffman MR, Ciucci MR, Jiang JJ, McCulloch TM. Automated analysis of pharyngeal pressure data obtained with high-resolution manometry. *Dysphagia* 2011;26:3-12. doi:[10.1007/s00455-010-9320-2](https://doi.org/10.1007/s00455-010-9320-2)
 19. Geng Z, Hoffman MR, Jones CA, McCulloch TM, Jiang JJ. Three-dimensional analysis of pharyngeal high-resolution manometry data. *Laryngoscope* 2013;123:1746-1753. doi:[10.1002/lary.23987](https://doi.org/10.1002/lary.23987)
 20. Mielens JD, Hoffman MR, Ciucci MR, McCulloch TM, Jiang JJ. Application of classification models to pharyngeal high-resolution manometry. *J Speech Lang Hear Res* 2012;55:892-902. doi:[10.1044/1092-4388\(2011/11-0088\)](https://doi.org/10.1044/1092-4388(2011/11-0088))
 21. Jell A, Kuttler C, Ostler D, Hüser N. How to Cope with Big Data in Functional Analysis of the Esophagus. *Visc Med* 2020;36:439-442. doi:[10.1159/000511931](https://doi.org/10.1159/000511931)
 22. Hoffman MR, Mielens JD, Omari TI, Rommel N, Jiang JJ, McCulloch TM. Artificial neural network classification of pharyngeal high-resolution manometry with impedance data. *Laryngoscope* 2013;123:713-720. doi:[10.1002/lary.23655](https://doi.org/10.1002/lary.23655)
 23. Lee TH, Lee JS, Hong SJ, et al. High-resolution manometry: reliability of automated analysis of upper esophageal sphincter relaxation parameters. *Turk J Gastroenterol* 2014;25:473-480. doi:[10.5152/tjg.2014.8021](https://doi.org/10.5152/tjg.2014.8021)
 24. Jungheim M, Busche A, Miller S, Schilling N, Schmidt-Thieme L, Ptok M. Calculation of upper esophageal sphincter restitution time from high resolution manometry data using machine learning. *Physiol Behav* 2016;165:413-424. doi:[10.1016/j.physbeh.2016.08.005](https://doi.org/10.1016/j.physbeh.2016.08.005)